Superconducting high-pressure phase of cesium iodide

Ying Xu,[1] John S. Tse,[1,2] Artem R. Oganov,[3,4] Tian Cui,[1] Hui Wang,[1] Yanming Ma,[1,*] and Guangtian Zou[1]
[1]*National Lab of Superhard Materials, Jilin University, Changchun 130012, People's Republic of China*
[2]*Department of Physics and Engineering Physics, University of Saskatchewan, Saskatoon, Saskatchewan, Canada S7N 5E2*
[3]*Department of Materials, Laboratory of Crystallography, ETH Zurich, HCI G 515, Wolfgang-Pauli-Strasse 10, CH-8093 Zurich, Switzerland*
[4]*Department of Geology, Moscow State University, 119992 Moscow, Russia*
(Received 2 March 2009; published 8 April 2009)

The evolutionary methodology for crystal structure prediction is employed to resolve a long-held puzzle in the high-pressure crystallography of cesium iodide. Above 42 GPa, an orthorhombic *Pnma* structure with a hexagonal-closed-packed (hcp) stacking which resembles hcp Xe is uncovered to be stable and successfully explains the observed diffraction patterns. At strong compression (>100 GPa), this structure becomes metallic via band-gap closure, and superconducting originated from the peculiar reverse electron donation from I^- to Cs^+.

DOI: 10.1103/PhysRevB.79.144110 PACS number(s): 74.62.Fj, 61.50.Ks, 74.25.Jb

I. INTRODUCTION

Cesium iodide (CsI) has long been a prototype system for high-pressure investigations due to the wide variety of phenomena it exhibits on compressions. As the most compressible alkali halide with a smallest band gap, it is a favorable material for the study of metallization. Contrary to most other alkali halides, CsI has the simple *CsCl* structure at ambient pressure and undergoes rather complicated transitions to low symmetric phases at high pressures. Moreover, CsI is isoelectronic with rare-gas solid Xe, and there exists the close similarity between CsI and Xe (Ref. 1) in the x-ray diffraction (XRD) patterns and the equations of state (EOS) at high pressures (>100 GPa). Interestingly, CsI metallizes at 115 GPa and becomes a superconductor above 180 GPa.[2,3] This observation leads to the important question on the underlying mechanism of the (super)conductivity in the very high-density state.[4] Two relevant earlier theoretical works[5,6] have explored the metallization; unfortunately, owing to the lack of information on high-pressure crystal structures, a full understanding of these intriguing phenomena was still not possible.

Earlier experiments suggested that CsI first undergoes a tetragonal[7–11] distortion at 40 GPa and then transforms to an orthorhombic structure[9,10] at 56 GPa. However, it was later shown that CsI has a continuous distortion from *CsCl* to orthorhombic at 45 GPa and then to a hcp-like phase.[1,12] The most characteristic difference is the quintuplet set of diffraction patterns below 100 GPa observed by Mao and co-workers,[1,12] which cannot be fit with the tetragonal and orthorhombic structures suggested earlier. At higher pressure, the quintuplet evolves into a triplet which is similar to that of hcp Xe. The cubic-to-orthorhombic transition is further confirmed by a subsequent experiment[13] and a theoretical calculation.[14] It was suggested[14] that the cubic-to-orthorhombic transition is driven by the softening of an acoustic phonon at the *M* point. Although these experimental[1,7–13] and theoretical[14,15] studies have been devoted to understanding the pressure-induced phase transitions in CsI, its full high-pressure structural information is still far from being clear and well established.

Here, we present extensive structure searches to uncover the high-pressure structures of CsI using the developed *ab initio* evolutionary algorithm.[16–18] This approach has been successful in the study of other materials at high pressure.[17–20] We have revealed an orthorhombic *Pnma* structure to be stable above 42 GPa, with which all the experimental structural data up to 300 GPa are explained. At higher densities, this structure becomes metallic and superconducting driven by the peculiar reverse electron donation from I^- to Cs^+.

II. COMPUTATIONAL DETAILS

Evolutionary search of high-pressure structures in CsI was performed with the evolutionary algorithm[16–18] in conjunction with *ab initio* structure relaxations within the framework of density-functional theory and the projector augmented wave (PAW) method[21,22] as implemented in the VASP code.[23] The evolutionary algorithm employed here was designed to search for the structure possessing the lowest free energy at given P/T conditions. The significant feature of this methodology is the capability of predicting the stable structure with only the knowledge of the chemical composition. The PAW potentials used here were derived using the generalized gradient approximation (GGA) (Ref. 24) functional and have [Pd] core (radius of 2.5 and 2.3 a.u.) for Cs and I. The use of a plane-wave kinetic-energy cutoff of 380 eV was shown to give excellent convergence on the total energies and structural parameters. Electron-phonon coupling (EPC) calculations have been performed using the pseudopotential plane-wave method and density-functional perturbation theory[25,26] as implemented in the QUANTUM-ESPRESSO package.[27] Norm-conserving scheme was used to generate the Perdew-Burke-Ernzerhof GGA density functional[24] pseudopotentials for Cs and I with the choices of electronic configurations of $5s^25p^66s^1$ and $5s^25p^5$, respectively. EPC calculation has been performed on a $4\times4\times4$ Monkhorst-Park (MP) (Ref. 28) *q*-point mesh in the first Brillouin zone. A $14\times14\times14$ MP *k* mesh is chosen to en-

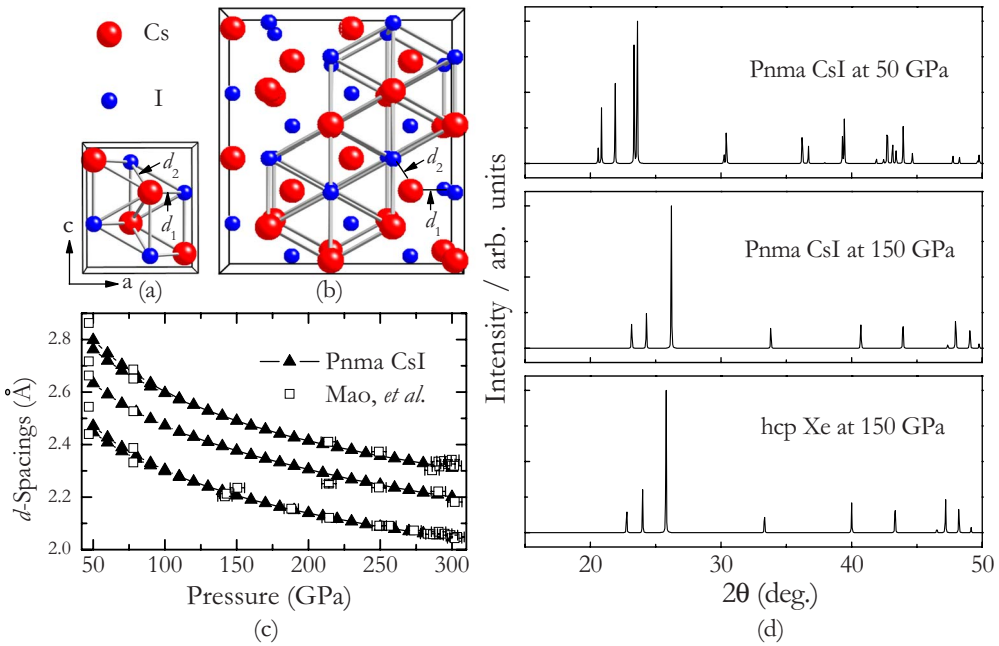

FIG. 1. (Color online) (a) Primitive cell of orthorhombic *Pnma* structure. (b) Top view of the *Pnma* structure ($2\times1.5\times2$ supercell) along b axis. At 100 GPa, the lattice parameters of *Pnma* structure are a=5.2091 Å, b=4.9458 Å, and c=5.9890 Å. Atoms occupy the Wyckoff 4c sites $(x,0.25,z)$ with x=0.58731 and z=0.37578 for Cs, and with x=0.58471 and z=0.87561 for I, respectively. The distances of d_1 and d_2 denote the nearest Cs-I bond lengths between two neighboring AB layers along a and c directions, respectively. (c) Simulated interplanar spacings for *Pnma* CsI as a function of pressure (solid up triangles) to compare with the experimental data (open squares) from Refs. 1 and 12. The lines are guides to the eyes. Below 110 GPa, the d spacings of quintuplet set of diffraction peaks were calculated from 020, 210, 002, 021, and 211, while those of triplet between 120 and 190 GPa are from 200, 020, and 210, and above 190 GPa from 210, 002, and 211. (d) Simulated XRD patterns of *Pnma* CsI at 50 and 150 GPa, and hcp Xe at 150 GPa shown from top to bottom panels.

sure k-point sampling convergence with Gaussians of 0.03 Ry, which approximates the zero-width limit in this calculation.

III. RESULTS AND DISCUSSION

Evolutionary variable-cell simulations with 2, 3, 4, and 8 formula units (f.u.) in the unit cell were performed at 5, 30, 41, 50, 100, and 300 GPa, respectively. In agreement with experiments,[1,7–13] simulations at 5 and 30 GPa reproduced correctly the *CsCl* structure as most stable. An orthorhombic structure with *Pmma* symmetry was found at 41 GPa. This structure has 2 f.u./cell and is identical to that proposed by earlier calculations.[14,15] At 50, 100, and 300 GPa, an orthorhombic *Pnma* structure having 4 f.u./cell [Fig. 1(a)] is found to be stable. A striking feature of this modification is that Cs and I atoms are packed in an hcp-like structure [Fig. 1(b)] with the stacking order along crystallographic b axis to be $ABAB\ldots$. The pattern of Cs-I ordering is nontrivial and displays clear geometrical frustration. At 100 GPa, the enthalpy of this hcp-like structure is 136.5 meV/f.u. lower than that of *Pmma* structure. The Cs-Cs bond lengths (3.009 Å) are nearly equal to those of I-I bonds (3.008 Å) within the pseudohexagons. The Cs-I bond length varies slightly from 2.988 to 3.012 Å within pseudohexagonal plane, close to the planar Xe-Xe distance (3.044 Å) in hcp Xe at the same pressure.[29] The distance between two neighboring A planes is 4.964 Å [Fig. 1(b)] and corresponds nicely to the c-lattice parameter of 4.994 Å in hcp Xe.[29] Moreover, geometric optimization of a model constructed by replacing Cs and I with Xe in *Pnma* structure arrived at the high-pressure hcp phase of Xe. However, the orthorhombic *Pnma* phase is characterized by two different nearest Cs-I bond lengths of d_1 and d_2 [Figs. 1(a) and 2] to make it distinct with hcp structure. At 50 GPa, d_1 (3.182 Å) is smaller than d_2 (3.244 Å) by about 0.062 Å. With increasing pressure d_1 and d_2 converges gradually. Specifically, the difference between d_1 and d_2 decreases to 0.019 Å at 110 GPa and 0.002 Å at 170 GPa [Fig. 2]. As d_1 and d_2 converges with pressure [Fig. 2], the *Pnma* structure resembles more with hcp. Enthalpy curves

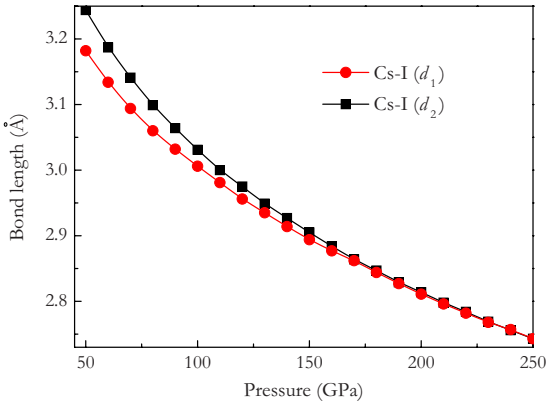

FIG. 2. (Color online) Pressure dependence of the nearest Cs-I bond lengths (d_1 and d_2) between two neighboring AB layers.

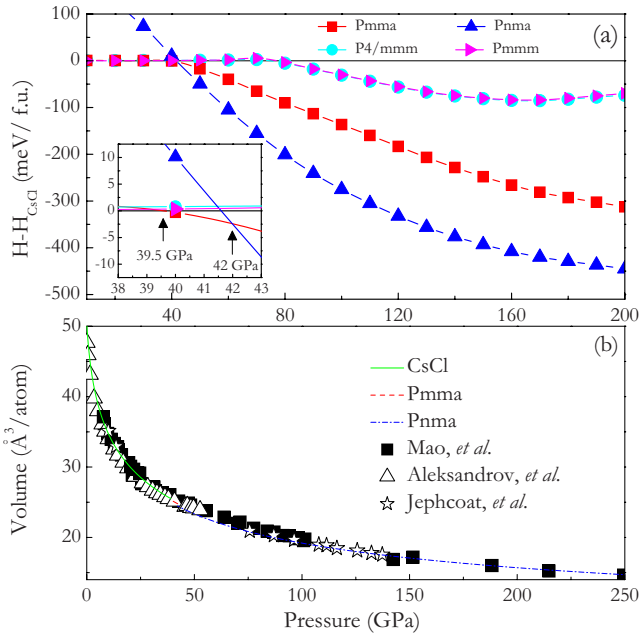

FIG. 3. (Color online) (a) Enthalpies (relative to the *CsCl* phase) of *Pmma* (solid squares), *Pnma* (solid up triangles), *P*4/*mmm* (solid circles), and *Pmmm* (from Ref. 6, solid right triangles) structures as a function of pressures. Structural optimizations were performed with a stringent energy convergence tolerance of 1×10^{-5} eV. Particular care has been taken to ensure the static total-energy convergence. Specifically, the plane-wave cutoff of 380 eV was used for all structures, and the *k* point sets for *CsCl*, *Pmma*, *Pnma*, *P*4/*mmm*, and *Pmmm* are chosen to be $8\times8\times8$, $12\times12\times12$, $8\times8\times8$, $12\times12\times12$, and $14\times14\times14$, respectively. Note that the enthalpies of *P*4/*mmm* and *Pmmm* structures are nearly identical. It is not surprising since the stacking order of Cs and I atoms in these two structures are rather similar. (b) Theoretical equation of states of *CsCl* (solid line), *Pmma* (dashed line), and *Pnma* (dash-dotted line) structures of CsI. The solid squares and open up triangles are the measured data for CsI from Refs. 1, 12, and 13. The open stars are the experimental data for solid Xe from Ref. 30.

for various structures are shown in Fig. 3(a). The transformation of *CsCl*→*Pmma* is predicted at 39.5 GPa, in good agreement with experiments[1,12,13] and earlier theoretical calculations.[14,15] However, *Pmma* structure is only stable in a very narrow pressure region of 39.5–42 GPa, above which *Pnma* structure becomes favorable and remains to be stable up to at least 300 GPa. Lattice dynamics calculations with no imaginary phonon frequencies support the dynamic stability of *Pmma* and *Pnma* structures over the pressure range studied here.

The pressure dependence of interplanar spacings of the XRD peaks at low diffraction angle (<30°) in *Pnma* structure is plotted in Fig. 1(c) to compare with the experimental data.[1,12] Because of the small Miller indices and large *d* spacing, this region is critical for structure assignment. Remarkably, all the experimental data in the pressure range of 50–300 GPa are successfully explained by the current structural model. Specifically, the diffraction peaks of *Pnma* structure at low pressures [Fig. 1(d)] exhibits a quintuplet feature at low diffraction angle, consistent with experimental observations which characterize an orthorhombic structure. With increasing pressure, the two double peaks of the quintuplet eventually merged together into two single peaks of a triplet [Fig. 1(d)]. This triplet represents an hcp-like structure as suggested by Mao and co-workers.[1,12] Note that the evolution of the quintuplet into the triplet at about 110 GPa [Fig. 1(c)] is closely related to the convergence of d_1 and d_2 [Fig. 2] as there is no such clear change in other nearest Cs-I separations in *Pnma* structure. EOS calculations [Fig. 3(b)] for the transition sequence of *CsCl*→*Pmma*→*Pnma* revealed an excellent agreement with experiments.[1,12,13] These two phase transitions can be both characterized as first order but with very small volume reduction of 0.7% and 1.3%, respectively. This explains the nearly continuous experimental EOS data. The experimental data[30] of hcp Xe are also presented in Fig. 3(b) for comparison. Interestingly, we found that above 75 GPa, the compression behavior of *Pnma* CsI is nearly identical to that in hcp Xe. This fact is consistent with the experimental observation.[1]

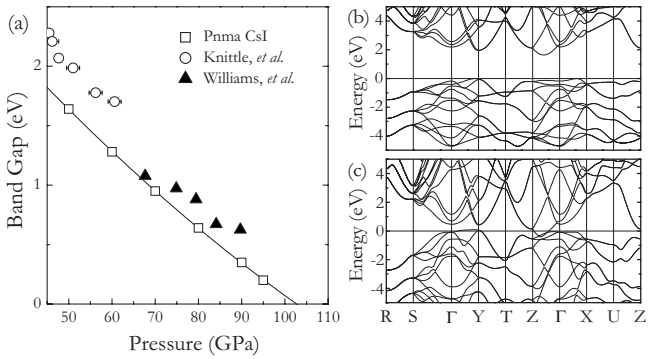

FIG. 4. (a) Pressure dependence of theoretical band gaps in *Pnma* CsI (open squares). The solid line is a linear fit. The open circles and solid up triangles are the experimental data from Refs. 7 and 31, respectively. Electronic band plots along high-symmetry directions of *Pnma* CsI at (b) 50 and (c) 120 GPa, respectively.

The pressure dependence on the band gap of *Pnma* CsI is compared with the optical experimental data[7,31] in Fig. 4(a). Extrapolation of the band-gap energy to zero value yields a metallization pressure of 103 GPa, in excellent agreement with 115 GPa obtained from direct electrical transport measurements.[3] The slightly smaller metallization pressure in theory is not unexpected due to the well-known band-gap underestimation by density-functional theory. The metallization of *Pnma* CsI occurs via indirect band-gap closure along the *Z*-Γ and Γ-*Y* directions [Figs. 4(b) and 4(c)], which is apparently contrasted to previous results of direct band-gap closure at the Γ point in Refs. 5 and 6. This big discrepancy is understandable since these earlier studies[5,6] did not adopt the appropriate high-pressure structure: Aidun *et al.*[5] simply took the zero-pressure *CsCl* structure and Satpathy *et al.*[6] used the orthorhombic *Pmmm* structure, whose enthalpy is much higher than the *Pnma* structure above 42 GPa [Fig. 3(a)]. As a result, the metallization pressure of 65 GPa predicted by Satpathy *et al.*[6] is too small to compare with the experimental data (115 GPa).[3] Band-gap closure of *Pnma* CsI between I 5*p* and Cs 5*d* bands results in a peculiar reverse electron donation from I^- to Cs^+, and the formation of

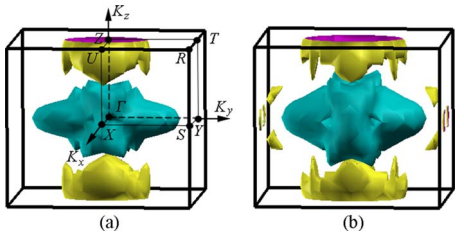

FIG. 5. (Color online) Fermi surfaces of *Pnma* CsI at (a) 160 and (b) 180 GPa, respectively.

several electron and hole Fermi-surface pockets [Figs. 4(b) and 4(c)]. With the pressure increasing, this intriguing $I^- \rightarrow Cs^+$ charge transfer becomes more significant and consequently, the Fermi surface at 180 GPa turns to be particularly rich and complex in comparison with that at 160 GPa due to a dramatic increase in the electron donation from I^- to Cs^+ [Fig. 5]. These additional Fermi sheets suggest that more electrons are involved in the EPC necessary for superconducting. This correlates nicely with the experimental observation of superconductivity only at very high pressure (~180 GPa).[2] The electronic band [Figs. 4(b) and 4(c)] crossing Fermi level along the Z-Γ direction is highly dispersive while it is quite flat (flatband refers to a section of a band within a narrow energy window centered at the Fermi level where the group velocities of the electrons approach zero) along Γ-Y and Γ-X. These electronic features apparently satisfy the "flatband-steep band" scenario, which has been suggested to be a favorable condition for the occurrence of superconductivity.[32]

Figure 6 shows the phonon density of states (DOS) and Eliashberg spectral function $\alpha^2F(\omega)$ (Ref. 33) for *Pnma* CsI at 180 GPa. It is found that $\alpha^2F(\omega)$ is strongly localized within a narrow vibrational region of 4.5–8 THz, where the integrated EPC λ is 0.1667 constituting 64% of the total λ, 0.2618. This suggests a strong anisotropic EPC behavior in *Pnma* structure and resembles that in hcp Xe.[29] With increasing pressure to 216 GPa, λ was reduced to be 0.257. The superconducting critical temperature (T_c) can be estimated from the Allen-Dynes modified McMillan equation[34] $T_c = \frac{\omega_{\log}}{1.2}\exp[-\frac{1.04(1+\lambda)}{\lambda-\mu*(1+0.62\lambda)}]$, where $\omega_{\log}$ is the logarithmic average frequency calculated directly from the phonon spectrum and μ^* is the Coulomb pseudopotential. $\omega_{\log}$ is obtained to be 285.13 K at 180 GPa and 313.83 K at 216 GPa. Using a μ^* of 0.1, the estimated T_c is 0.03 K at 180 GPa but is reduced to be 0.025 K at 216 GPa. This naturally explains the experimental observation[2] of T_c reduction with pressure. The projected phonon DOSs for Cs and I atoms are nearly identical

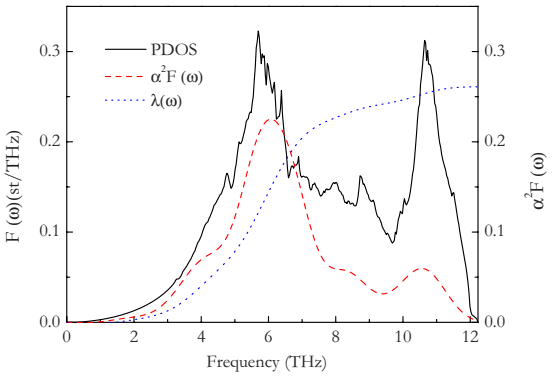

FIG. 6. (Color online) The calculated phonon density of states (solid line), Eliashberg spectral function $\alpha^2F(\omega)$ (dashed line), and the electron-phonon integral λ(ω) (dotted line) of *Pnma* CsI at 180 GPa.

showing that both atoms contribute equally to the EPC. Owing to the small difference in the atomic mass of Cs, I, and Xe atoms, EPC mechanism of *Pnma* CsI and hcp Xe may be viewed as nearly equal. Indeed, the estimated T_c is 0.04 K at 215 GPa for hcp Xe.[29] However, the estimated T_c in CsI is noticeably smaller than the experimental value[2] (e.g., at 216 GPa, theoretical value of 0.025 K vs experimental value of 1.3 K). It is noteworthy that conventional one band theory (i.e., averaging of coupling strengths) adopted in this theory might be insufficient to describe the transition temperature for an anisotropic EPC system.[35] Perhaps, a more accurate theoretical method is needed in order to reproduce the experimental T_c.

IV. CONCLUSIONS

In summary, we have employed the evolutionary algorithm to predict the high-pressure crystal structures of CsI. A high-pressure orthorhombic *Pnma* structure has been uncovered to be stable above 40 GPa and exist at least up to 300 GPa. Within the *Pnma* structure, the experimental XRD data and the converged EOS of CsI and Xe above 100 GPa are well understood. We further discovered that *Pnma* CsI metallizes as a result of indirect band overlap. This creates a peculiar reverse electron donation from I^- to Cs^+, responsible for the superconductivity in CsI at 180 GPa.

ACKNOWLEDGMENTS

We thank the financial support from the China 973 Program under Grant No. 2005CB724400, the National Natural Science Foundation of China under Grant No. 10874054, the NSAF of China under Grant No. 10676011, and the 2007 Cheung Kong Scholars Programme of China.

*Author to whom correspondence should be addressed; mym@jlu.edu.cn

[1] H. K. Mao, Y. Wu, R. J. Hemley, L. C. Chen, J. F. Shu, and L. W. Finger, Science **246**, 649 (1989).
[2] M. I. Eremets, K. Shimizu, T. C. Kobayashi, and K. Amaya, Science **281**, 1333 (1998).
[3] M. I. Eremets, K. Shimizu, T. C. Kobayashi, and K. Amaya, J. Phys.: Condens. Matter **10**, 11519 (1998).
[4] R. J. Hemley, Science **281**, 1296 (1998).
[5] J. Aidun, M. S. T. Bukowinski, and M. Ross, Phys. Rev. B **29**, 2611 (1984).
[6] S. Satpathy, N. E. Christensen, and O. Jepsen, Phys. Rev. B **32**,

6793 (1985).
[7] E. Knittle and R. Jeanloz, Science **223**, 53 (1984).
[8] T.-L. Huang and A. L. Ruoff, Phys. Rev. B **29**, 1112 (1984).
[9] K. Asaumi, Phys. Rev. B **29**, 1118 (1984).
[10] Y. K. Vohra, S. T. Weir, K. E. Brister, and A. L. Ruoff, Phys. Rev. Lett. **55**, 977 (1985).
[11] Y. K. Vohra, K. E. Brister, S. T. Weir, S. J. Duclos, and A. L. Ruoff, Science **231**, 1136 (1986).
[12] H. K. Mao, Y. Wu, R. J. Hemley, L. C. Chen, J. F. Shu, L. W. Finger, and D. E. Cox, Phys. Rev. Lett. **64**, 1749 (1990).
[13] I. V. Aleksandrov, A. F. Goncharov, I. N. Makarenko, and S. M. Stishov, Phys. Rev. B **43**, 6194 (1991).
[14] M. Buongiorno Nardelli, S. Baroni, and P. Giannozzi, Phys. Rev. Lett. **69**, 1069 (1992).
[15] B. Winkler and V. Milman, J. Phys.: Condens. Matter **9**, 9811 (1997).
[16] C. W. Glass, A. R. Oganov, and N. Hansen, Comput. Phys. Commun. **175**, 713 (2006).
[17] A. R. Oganov and C. W. Glass, J. Chem. Phys. **124**, 244704 (2006).
[18] A. R. Oganov, C. W. Glass, and S. Ono, Earth Planet. Sci. Lett. **241**, 95 (2006).
[19] Y. Ma, A. R. Oganov, and Y. Xie, Phys. Rev. B **78**, 014102 (2008).
[20] Y. Ma, A. R. Oganov, and C. W. Glass, Phys. Rev. B **76**, 064101 (2007).
[21] P. E. Blöchl, Phys. Rev. B **50**, 17953 (1994).
[22] G. Kresse and D. Joubert, Phys. Rev. B **59**, 1758 (1999).
[23] G. Kresse and J. Furthmüller, Phys. Rev. B **54**, 11169 (1996).
[24] J. P. Perdew, K. Burke, and M. Ernzerhof, Phys. Rev. Lett. **77**, 3865 (1996).
[25] S. Baroni, P. Giannozzi, and A. Testa, Phys. Rev. Lett. **58**, 1861 (1987).
[26] P. Giannozzi, S. de Gironcoli, P. Pavone, and S. Baroni, Phys. Rev. B **43**, 7231 (1991).
[27] A. D. C. S. Baroni, S. de Gironcoli, P. Giannozzi, C. Cavazzoni, G. Ballabio, S. Scandolo, G. Chiarotti, P. Focher, A. Pasquarello, K. Laasonen, A. Trave, R. Car, N. Marzari, and A. Kokalj, http://www.pwscf.org.
[28] H. J. Monkhorst and J. D. Pack, Phys. Rev. B **13**, 5188 (1976).
[29] Y. Yao and J. S. Tse, Phys. Rev. B **75**, 134104 (2007).
[30] A. P. Jephcoat, H.-k. Mao, L. W. Finger, D. E. Cox, R. J. Hemley, and C.-s. Zha, Phys. Rev. Lett. **59**, 2670 (1987).
[31] Q. Williams and R. Jeanloz, Phys. Rev. Lett. **56**, 163 (1986).
[32] A. A. Simon, Angew. Chem., Int. Ed. Engl. **36**, 1788 (1997).
[33] P. B. Allen, Phys. Rev. B **6**, 2577 (1972).
[34] P. B. Allen and R. C. Dynes, Phys. Rev. B **12**, 905 (1975).
[35] W. Pickett, Nature (London) **418**, 733 (2002).